



# A kinematic model for folds accommodating shortening in tips of reverse faults: an example from the southern Pyrenees (N Iberian Peninsula)

H. UZKEDA<sup>1</sup>\*, J. POBLET<sup>1</sup> AND M. BULNES<sup>1</sup>

<sup>1</sup>*Departamento de Geología, Universidad de Oviedo, C/Jesús Arias de Velasco s/n, 33005 Oviedo, Spain.*

\**e-mail: hodei@geol.uniovi.es*

---

**Abstract:** A kinematic model for fault-related folds is proposed based on a field example from the Pyrenees. A brief explanation of the model with remarks on its properties and why it was chosen to simulate the natural structure is given together with a detailed structural analysis. The structure consists of a meter-scale fold developed at the tip of a thrust fault with its backlimb dipping less than the fault surface and including a footwall fold. The suggested model presents an acceptable geometrical fitting to the studied structure and provides a reasonable evolutionary history for the fold. Graphs of shortening vs. slip along the fault can be obtained using the model's equations in which a possible structural path followed by the structure can be depicted.

**Keywords:** thrust-related fold, southern Pyrenees, kinematic model, shortening, structural relief.

---

A natural fault-related fold that crops out at the trench of a local road in the southern Pyrenees was studied in detail (Fig. 1). This natural example has been selected because of the good quality outcrop, excellent accessibility, stratigraphy and easy to identify structures, and because most of the structure is exposed, thus minimizing the extrapolation required to complete the subsurface part.

At first glance, the studied structure looks like a simple fault-propagation fold related to a thrust but, when analysed in more detail, problems arise when trying to interpret it by using the classical models for fault-propagation folds proposed in the literature. These discrepancies led us to develop a new kinematic model that could explain the features seen in the field (Fig. 2). The resultant model is similar to those previously proposed by McConnell *et al.* (1997) and Tavani *et al.* (2006), with a double-edge propagating fault, not necessarily joined to a detachment level. The main properties and characteristics of the model are: a) reverse fault not joined to a detachment, b)

fault oblique to the fold limbs, c) folds developed in both the footwall and the hangingwall, d) fault nucleating in a point and propagating stratigraphically upwards and downwards symmetrically in the simplest model, e) folding accommodating the whole shortening in the beds close to, but not affected by the fault tip, and part of it in the beds offset by the fault, and f) slip decreasing from the fault's midpoint to the tips of the fault (Fig. 2).

When trying to simulate a natural structure using this model there are two end members that would supply the same final result: a) the fault is already propagated, i.e. the fault acquired its ultimate length at time step 0. The slip increases while the fault length remains constant; it could be considered that the fault propagation-to-slip ratio is equal to zero. In this situation the fold is amplified by limb rotation, so that the limb dip increases as the shortening rises, b) the fault propagation-to-slip ratio is constant at every moment and is equal to the ratio that can be measured at the present, deformed state. As the shortening



**Figure 1.** Interpreted photograph of the structure under investigation displaying the stratigraphic levels (I-XI) identified in the field and the beds used to construct the profile (1-10).

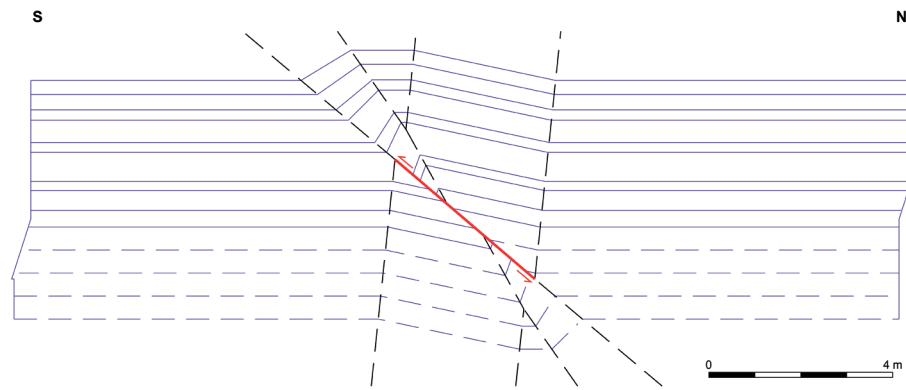


**Figure 2.** Kink-like model developed to simulate the studied field structure. The main features are depicted in this figure: fault not joined to a detachment; backlimb dipping less than the fault; structures in both the footwall and hangingwall. The dashed lines are the beds located under the topographic surface.

increases, the fold amplifies, conserving the limbs' dips which were acquired "instantaneously" at time step 0 and remained constant during the whole process, i.e. the fold amplifies by hinge migration.

### Geological setting

The studied structure is located in the Pyrenees. The Pyrenees are an approximately E-W-trending Alpine cordillera that resulted from collision of the Iberian and the Euroasian plate from Late Cretaceous to Miocene times (e.g. Muñoz, 1992). This collision caused inversion tectonics of previous extensional basins of Permian-Triassic-Cretaceous age and involved the old Paleozoic basement, deformed during the Variscan orogeny. The resulting cordillera is an asymmetrical elongated belt traditionally divided in three different zones: the North Pyrenean Zone, the Axial Zone and the South Pyrenean zone (Seguret, 1972).

The chosen structure is located in the western part of the South Pyrenean Zone, close to the boundary with the Axial Zone, within the structural unit called "Lower Thrust Sheets" (Muñoz, 1992). This unit is constituted by nappes that include materials from the basement as well as the sedimentary cover. The latter is characterized by a reduced Mesozoic sequence and thick Paleogene series, whose lower part would represent the depositional sequence of the South Pyrenean Foreland. This unit presents a wide variety of thrust system types: imbricated systems in the external zones and duplexes and antiformal stacks in the internal portion (García and Martínez, 1994). The fault-propagation fold analysed crops out along a trench of the road that connects the localities of Zubiri and Eugi, located in Navarre.

### Stratigraphy

The materials involved in the structure investigated are decimetric to metric alternations of marls and

limestones with an age from Thanetian to Ypresian (Paleocene-Eocene) (Carbayo *et al.*, 1978). There are numerous sedimentary structures: flute and bounce casts, parallel lamination and current ripples. The strata show, in general, tabular geometries, with erosive bases that, in some cases, may be channelized. The limestones/marls ratio is high, the presence of amalgamated limestones being common. These have been interpreted as the infill of a turbiditic trench fed by denudation of carbonate shelves (García and Martínez, 1994). In the studied structure eleven stratigraphic levels (I-XI) of marls and limestones were identified (Fig. 1).

### Structural features

The studied example consists of a reverse fault offsetting several beds and folds possibly related to the movement along the fault (Fig. 1).

The fault is a roughly planar surface with a dip of between 40° and 50° to the north. There is also another fault, more or less parallel to the main one, which cuts and offsets limestone level IV and folds the underlying massive limestones. These two faults are reverse and S-directed, in accordance with observations on a regional scale. The mean dip direction of the kinematic indicators measured on the fault plane is around N5E with a dip of 35°, pointing to a dip-slip movement. The slip is maximum in the middle portion of the main fault (1.2 m measured) and decreases towards the fault tips.

The fold above the fault tip is asymmetric, with the backlimb (northern) less inclined than the forelimb (southern). In general, beds have an approximately E-W strike, with gentle dips to the north, except those measured in the frontal limb of the fold, where the strata dip to the south with higher values that decrease from the lower to the upper beds. In the backlimb,

beds dip less than the fault. The axes of both the major and the minor folds tend to be subhorizontal with a strike approximately E-W, in accordance with the main direction of folding in the region (Carbayo *et al.*, 1978; García and Martínez, 1994). The asymmetry of some minor and major folds indicates a south vergence, which is consistent with the thrust displacement sense.

The strata display a thickening in the front limb that is more notorious in level VIII and the marls above it. The way the beds accommodate this thickening depends on their lithological properties; the marls, more plastic, underwent ductile processes, whereas the more competent calcarenite (level VIII) exhibits faults that increased its thickness.

The foliation surfaces possess a strike almost parallel to that of the stratification. These planes present generally high dips, most of them over  $55^\circ$ , towards the north. The development of this foliation is strongly conditioned by the lithology. For example, it is absent within the calcarenites, whereas the marls, especially level V and, more notably, next to the fold core, are intensely foliated. The intersection lineation between the stratification and the foliation is almost parallel to the direction of the fold axes. Both axial planes of the major and minor folds and foliation steeply dip to the north, suggesting that it is an axial plane foliation.

The presence of joints, mainly developed in the beds formed by massive limestones such as levels I, III or VII, is remarkable. These joints are subvertical planes, striking approximately ENE-WSW.

### Construction of a geological profile

A section across the structure investigated was constructed using various sources of data: a) a geological interpretation of photographs that were taken as per-

pendicular as possible to the outcrop and to the fold axis (Fig. 1), b) a laser-rangefinder to obtain a dataset of 3D coordinates of the features seen in the photographs (Xu *et al.*, 2000, 2001). For the sake of simplicity, a 3D local coordinates system was used. This allows us to correct possible photographic distortions and to construct a cross section perpendicular to the fold axis, projecting the data along the axis direction, c) finally, measurements of thicknesses, dips and strikes were taken in the field and utilised to constrain the thickness variations, beds and structure dips observed.

As a final result, a cross section approximately parallel to the transport direction (measured using kinematic indicators observable on the fault plane) and perpendicular to the fold axis was obtained. The direction chosen to construct this profile was N10W. This direction was selected after constructing  $\beta$  diagrams (Ramsay, 1967) for several beds and observing that the mean  $\beta$  axis had a strike of about N100W and an approximately horizontal dip (less than  $5^\circ$ ) (Fig. 3).

### Interpretation and subsurface reconstruction

After constructing the outcropping part of the structure, techniques that permit the calculation of the depth of the detachment (Chamberlin, 1910; Epard and Groshong, 1993) were used to attempt to reconstruct the subsurface section. One feature worth noting is that the footwall regional data, if taken as horizontal, seems to be elevated over the hangingwall regional data. There are several causes that could explain this fact. Among them, the most probable are: a) the presence of a structure that would lift the footwall beds and would be responsible for an incipient fold developed in levels III and IV in the southernmost part of the section, b) thickness changes, with a thicker footwall sequence, and c) regional data dipping to the north. The last explanation was chosen to

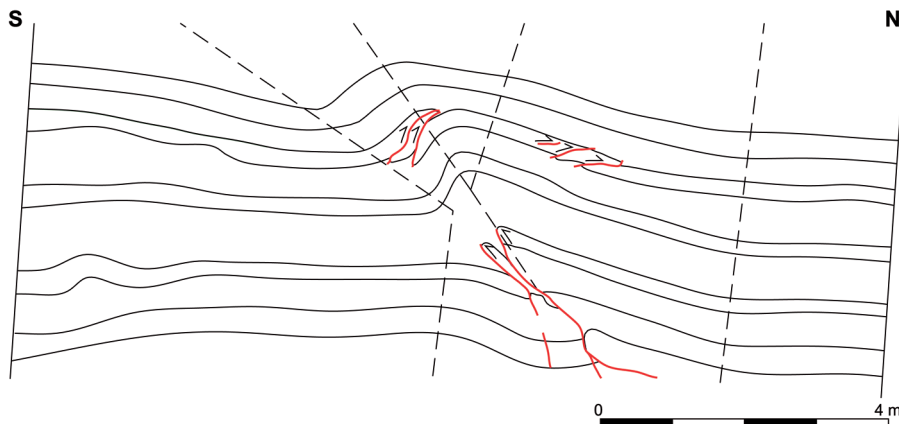


**Figure 3.** Geological cross section constructed perpendicular to the fold axis and parallel to tectonic transport (corresponds to the plane N10W).

make the different measurements (areas, lengths, elevation, etc.) needed for the depth to detachment and structural relief estimations. The Chamberlin method is problematic when used with the marly levels that do not preserve their lengths. Considering this limitation, the method would be suitable for the more competent levels, such as level VIII or IV, that suffered fragile deformation and that would have maintained their lengths. The results are, however, not completely satisfactory since the detachment should be visible in the outcrop. Neither using the method by Epard and Groshong (1993) are the results good. The fact that the results achieved using the methods to calculate the depths to detachment are not acceptable could be explained in the absence of a detachment level. This led us to use other types of technique to reconstruct the subsurface portion of the structure, such as identifying the type of fault-related fold.

According to all the data available, the fold could respond to three models of formation: a) a fault propagation fold with the backlimb not parallel to the fault, as the one described by Suppe and Medwedeff (1990). In this case, the fold would have developed over a thrust formed by at least two segments with different dip that might join a subsurface detachment level. However, the Suppe and Medwedeff model has an unavoidable problem, namely that the footwall is not deformed, whereas in our field example the footwall is folded; b) another possibility is that the fold was formed by a double edge propagating fault following a model similar to those proposed by McConnell *et al.* (1997) and Tavani *et al.* (2006). The fault would have a nucleation point from where it would propagate upwards and downwards. In this situation a detachment level would not be required. This model has the advantage that a fold would be developed in the footwall. In this model the fault can be considered to be previous to the folding, i.e. the fault propagates first and then the beds become folded, or it propagates simultaneously to the folding. The first assumption means that the fold was created by limb rotation and the axial planes associated with the fault did not migrate, only rotated. If the second statement is true, then the mechanism of fold amplification would be hinge migration first and finally, when the fault reaches its actual length, limb rotation would occur. The limb rotation, in the latter situation, is not absolutely necessary if the dips chosen for the back and the frontal limb are equal to the actual ones; c) the last option is a break-thrust fold. The fold would be formed and, in a later event, a fault would cut off some strata. The problem with this hypothesis is that when the fault movement is removed, a coherent fold can not be obtained.

For the above reasons, a model with a fault propagating from a nucleation point was preferred to simulate the natural structure investigated. The properties of this model adjust pretty well to the features that can be seen in the natural fold. The shortening history is different, depending on which fold amplification mechanism is chosen (hinge migration or limb rotation); these two end-members define a field which comprises all the possible evolutionary paths (Fig. 4).

### Analysis of shortening and crestal structural relief

The variation of the crestal structural relief for different stratigraphic horizons was estimated by separating the fraction caused by the fault and the fraction generated by folding. The proposed kinematic model can be used to estimate the structural relief for each bed. The actual and the calculated structural relief have similar behaviours; the relief increases upwards from the middle portion of the fault, up to the beds not affected by the fault which present a constant value. The relief varies from 0.40 m (0.41 m using the model) in the lower beds to 0.84 m (0.65 m using the model) in the upper ones (Fig. 5, Left).

Concerning the shortening, the layer parallel shortening and the curvilinear shortening were calculated. The former has larger values in the marly levels; these beds suffered ductile deformation which caused a loss

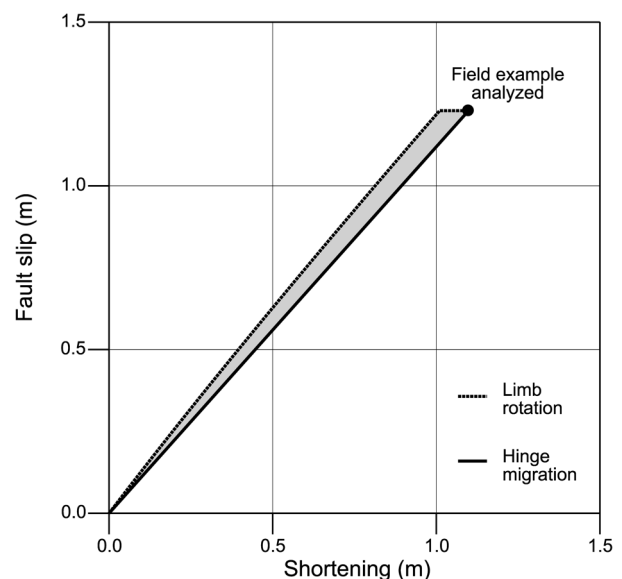


**Figure 4.** Slip vs. shortening graph for the kinematic model proposed. The shaded triangle formed by the limb rotation and hinge migration paths is the boundary for the different evolutionary paths foreseen by the model. The final fault slip and shortening correspond to those of the bed situated at the midpoint of the fault.

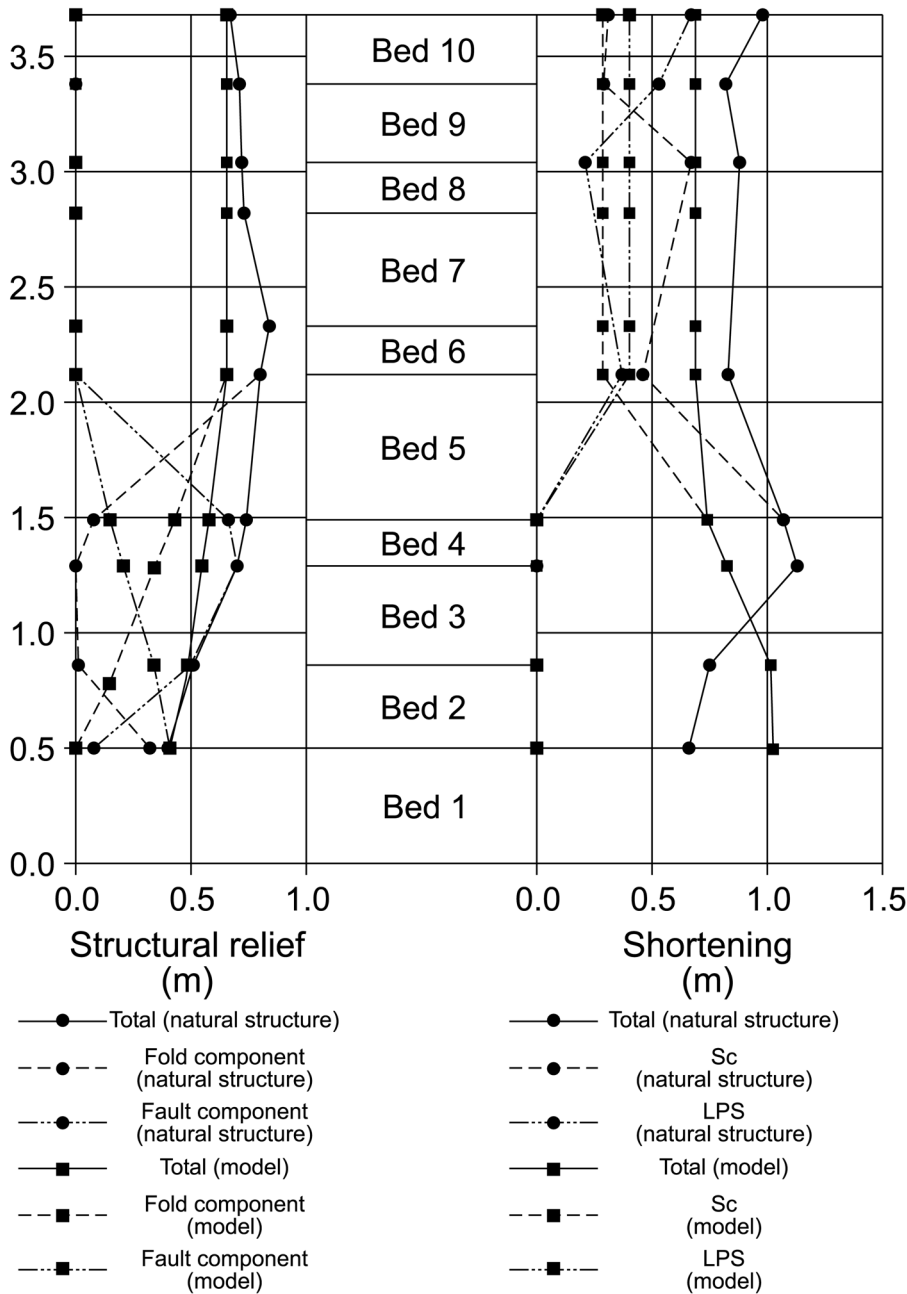


**Figure 5.** Left: graph of bed by bed structural relief separating the fault and the folding components, Right: graph of shortening separating the fraction caused by curvilinear shortening (Sc) and by layer parallel shortening (LPS). Both the actual and the calculated values using the model are plotted for each bed.

of bed length. In contrast, the more competent units, i.e. those presenting faults to accommodate shortening, exhibit values of layer-parallel shortening close to zero. Using the kinematic model a theoretical shortening can be calculated. The measured mean shortening is about 1 m (9%) whereas the obtained shortening using the model is slightly lower (0.78 m; 7%) (Fig. 5, Right).

**Conclusions**

A new kinematic model for thrust-related folds is proposed and applied to a natural example from the

Southern Pyrenees. The structure studied involves Cenozoic rocks and consists of a metric scale fold related to a reverse fault with the backlimb dipping less than the fault that can be adjusted by a model consisting of a double-edge propagating reverse fault not connected to a detachment.

Values of structural relief and shortening bed-by-bed have been obtained together with a likely evolution of the structure using the proposed model. The structural relief varies from 0.4 to 0.9 m and the mean shortening has a value of around 1 m (10%).

## Acknowledgements

We acknowledge financial support through projects CGL2005-02233/BTE (3D modelling of folding kinematic mechanisms), CGL2008-03786/BTE (mechanical analysis of deformation distribution in folds), CGL2006-12415-C03-02/BTE (Structural evolution of the Central Andes between parallels 23° and 33° during the Upper Paleozoic) and CSD2006-0041 (Topo-Iberia) under Consolider-Ingenio 2010 Programme funded by the

Spanish Ministry for Education and Science, CGL2008-00463-E/BTE (International Meeting of Young Researchers in Structural Geology and Tectonics) funded by the Spanish Ministry for Science and Innovation, and CNG08-15 (International Meeting of Young Researchers in Structural Geology and Tectonics -YORSGET-08-) funded by the Asturian Ministry for Science and Education. J. M. Casas's suggestions are gratefully acknowledged. We would like to thank the editors of this volume.

## References

- CARBAYO, A., DEL VALLE, J., LEÓN, L. and VILLALOBOS, L. (1978): *Mapa Geológico de España escala 1:50 000, Hoja 116 (Garralda)*. IGME.
- CHAMBERLIN, R. T. (1910): The Appalachian folds of central Pennsylvania. *J. Geol.*, 18, 3: 228-251.
- EPARD, J. L. and GROSHONG, R. H. (1993): Excess area and depth to detachment. *AAPG Bull.*, 77, 8: 1291-1302.
- GARCÍA, A. and MARTÍNEZ, L. M. (1994): *Mapa geológico de Navarra escala 1:25 000 Hoja 116-I (Erro)*. Nafarroako Foru Aldundia.
- MCCONNELL, D. A., KATTENHORN, S. A. and BENNER, L. M. (1997): Distribution of fault slip in outcrop-scale fault-related folds, Appalachian Mountains. *J. Struct. Geol.*, 19, 3-4: 257-267.
- MUÑOZ, J. A. (1992): Evolution of a continental collision belt-ECORS-Pyrenees crustal balanced cross-section. In: K. R. MCCLAY (ed): *Thrust tectonics*, Chapman and Hall, London: 235-246.
- RAMSAY, J. G. (1967): *Folding and fracturing of rocks*. Mc Graw-Hill, New York, 568 pp.
- SEGURET, M. (1972): *Etude tectonique des nappes et series decollees de la partie centrale du versant sud des Pyrenees; caractere synsedimentaire, role de la compression et de la gravite*. Montpellier: USTELA, 155 pp.
- SUPPE, J. and MEDWEDEFF, D. A. (1990): Geometry and kinematics of fault-propagation folding. *Eclogae Geol. Helv.*, 83, 3: 409-454.
- TAVANI, S., STORTI, F. and SALVINI, F. (2006): Double-edge propagation folding: geometry and kinematics. *J. Struct. Geol.*, 28, 1: 19-35.
- XU, X., AIKEN, C. L. V., BHATTACHARYA, J. P., CORBEANU, R. M., KENT, C., MCMEECHAN, G. A. and ABDELSALAM, M. G. (2000): Creating virtual 3-D outcrop. *The Leading Edge*, 19, 2: 197-202.
- XU, X., BHATTACHARYA, J. P., DAVIES, R. K. and AIKEN, C. L. V. (2001): Digital geologic mapping of the Ferron Sandstone, Muddy Creek, Utah, with GPS and reflectorless rangefinder. *GPS Solutions*, 19, 1: 15-23.